Biopolymer Chitosan-Activated Charcoal Adsorptive Composite Material: A Feasible Approach to Methylene Blue Dye Removal from Water

Arun Kumar Shukla , Javed Alam * , Janne Ruokolainen , Kavindra Kumar Kesari *

Posted Date: 5 October 2023

doi: 10.20944/preprints202310.0272.v1

Keywords: activated charcoal; chitosan; biopolymer; methylene blue; dye removal

Article

Biopolymer Chitosan-Activated Charcoal Adsorptive Composite Material: A Feasible Approach to Methylene Blue Dye Removal from Water

Arun Kumar Shukla [1], Javed Alam [1,*], Janne Ruokolainen [3] and Kavindra Kumar Kesari [2,3,*]

[1] College of science, King Saud University, P.O. Box 2455, Riyadh 11451, Saudi Arabia; ashukla@ksu.edu.sa, javaalam@ksu.edu.sa
[2] Research and Development Cell, Lovely Professional University, Phagwara, India; kavindra.kesari@aalto.fi
[3] Department of Applied Physics, School of Science, Aalto University, Espoo, Finland; janne.ruokolainen@aalto.fi, kavindra.kesari@aalto.fi
* Correspondence: javaalam@ksu.edu.sa (J.A), kavindra.kesari@aalto.fi (K.K.K)

Abstract: Water pollution, driven largely by the discharge of organic dyes from various industrial processes, presents a grave environmental threat. This study delves into the promise of an innovative adsorptive composite material composed of chitosan and activated charcoal, offering a sustainable and efficient solution for removing methylene blue (MB) dye from water sources. Our comprehensive investigation encompasses the synthesis, characterization, and adsorption capabilities of this composite material, revealing its remarkable physicochemical attributes and its substantial capacity to adsorb MB dye. These findings establish it as a compelling candidate for water treatment applications. The assessment of adsorbent dosage shows a direct correlation between higher dosages and enhanced MB dye removal, with an optimal dosage determined at 0.4 g/25 mL. Furthermore, pH-dependent studies demonstrate exceptional performance at lower pH levels, achieving an impressive 95% removal rate at pH 3 after 240 minutes of contact time. The composite exhibits consistent high removal percentages across a wide range of MB dye concentrations, showcasing its adaptability. In terms of reaction time, the composite achieves peak adsorption capacity within the initial 360 minutes and maintains a stable equilibrium, sustaining an impressive 99% removal efficiency thereafter. This study underscores the eco-friendliness and cost-effectiveness of the composite material, emphasizing its potential to address water pollution challenges and promote sustainable water resource management. Overall, this research yields valuable insights into a practical approach for mitigating the adverse impact of organic dyes on aquatic ecosystems and public health.

Keywords: activated charcoal; chitosan; biopolymer; methylene blue; dye removal

1. Introduction

The contamination of natural water resources by synthetic dyes has become a global concern, posing a significant threat to both aquatic ecosystems and human health [1]. Among these synthetic dyes, Methylene Blue (MB) stands out as a particularly notorious pollutant due to its widespread use in various industries, including textiles, printing, and dyeing. Characterized by its vibrant blue color and remarkable stability, MB has come to symbolize the environmental challenges linked to industrial wastewater discharge [2,3]. The unrestrained use of synthetic dyes in industrial processes has led to the release of a multitude of colorants into water bodies, precipitating severe environmental and health-related issues [4–7]. These synthetic dyes, including MB, are often non-biodegradable and exhibit a distressing persistence in water, rendering their removal a formidable endeavor [8,9]. In response to these challenges, diverse wastewater treatment strategies have been devised, such as coagulation, flocculation, oxidation, and membrane filtration [10–13]. While these methods offer

 doi:10.20944/preprints202310.0272.v1

some effectiveness, they often necessitate the use of chemical additives or energy-intensive processes, consequently contributing to secondary pollution and escalating operational costs [14].

In this context, adsorption-based techniques have arisen as an appealing alternative for the removal of synthetic dyes from water, offering simplicity, cost-effectiveness, and a minimal environmental footprint [15–18]. Activated charcoal, with its remarkable surface area and potent adsorption capacity, has garnered widespread recognition as an adsorbent material for dye removal. Nevertheless, practical applications of activated charcoal are hampered by challenges such as agglomeration, recovery difficulties, and the need for regeneration [19–21].

Concurrently, biopolymers have been gaining increased attention as environmentally friendly alternatives for water treatment applications [22]. Chitosan, a biopolymer derived from chitin, the second most abundant natural polymer after cellulose, has emerged as an attractive candidate owing to its exceptional adsorption properties, stemming from its amino and hydroxyl functional groups. Chitosan is biodegradable, non-toxic, and renewable, making it an appealing choice for developing adsorbent materials [23–26].

Chitosan, a linear polysaccharide composed of β-(1-4)-linked D-glucosamine and N-acetyl-D-glucosamine units, possesses unique properties that render it a versatile adsorbent material [24,27,28]. Its adsorption capabilities primarily arise from the abundance of amino and hydroxyl groups, allowing it to form hydrogen bonds with a wide spectrum of molecules, including dyes. In aqueous solutions with pH values below its pKa, the amine groups in chitosan become positively charged, augmenting its affinity for cationic dye molecules like MB [29]. Additionally, chitosan's inherent porous structure, derived from its natural polymer chains, provides a substantial surface area for dye adsorption [30,31]. This intrinsic porosity can be further enhanced through modifications, such as cross-linking, grafting, or blending with other materials, thereby improving its adsorption capacity and stability. The ease of functionalization allows researchers to tailor chitosan-based adsorbents to meet the specific requirements of various dye removal applications [31–34].

Activated charcoal, also known as activated carbon, represents a highly porous carbon material produced from various organic precursors such as coconut shells, wood, and agricultural waste [35,36] . The activation process involves heating the precursor material in the presence of an oxidizing agent or gas to create a network of pores and increase its surface area [37]. This results in a material with a vast number of active sites available for adsorption. The exceptional adsorption capacity of activated charcoal arises from its extensive internal surface area, typically ranging from 300 to 2,500 m^2/g, depending on the source material and activation method. These pores can adsorb a wide range of contaminants, including organic molecules, gases, and heavy metals. However, the use of activated charcoal in its raw form may be limited due to issues such as agglomeration, difficulty in recovery, and limited reusability [38].

To address these limitations and optimize the adsorption performance of activated charcoal, researchers have explored various modification techniques [39]. These modifications include chemical functionalization, blending with other materials, and immobilization onto solid supports. Such approaches aim to enhance the adsorption efficiency, improve selectivity, and facilitate the recovery and regeneration of the adsorbent material [40,41].

The combination of chitosan and activated charcoal in the form of a composite material leverages the unique properties of both components to create a synergistic adsorption system [42,43]. This synergy not only elevates the overall adsorption capacity but also mitigates issues related to the aggregation of activated charcoal particles [44,45]. Additionally, the immobilization of activated charcoal within the chitosan matrix facilitates the recovery and reusability of the adsorbent. Chitosan-activated charcoal composites have been explored in various environmental applications, including the removal of heavy metals, organic pollutants, and dyes from wastewater [46,47]. The selection of appropriate preparation methods, composite ratios, and activation techniques plays a crucial role in tailoring the composite material for specific adsorption tasks.

In light of these considerations, this study embarks on a comprehensive investigation into the development and application of a chitosan-activated charcoal adsorptive composite material for the efficient removal of MB dye from water. The research is driven by a set of specific objectives: to

 doi:10.20944/preprints202310.0272.v1

synthesize chitosan-activated charcoal composite materials with varying ratios, thus optimizing their efficacy in dye removal; to comprehensively characterize the physical, chemical, and structural properties of these composites using advanced techniques including Fourier-transform infrared spectroscopy (FTIR), X-ray photoelectron spectroscopy (XPS), and thermogravimetric analyzer (TGA); to rigorously evaluate the adsorption performance of these composite materials under various parameters, enabling a deep understanding of their capabilities; and to assess the reusability and regeneration potential of the composite materials, thereby contributing to sustainable and environmentally friendly approaches for dye removal from water systems.

2. Materials and Methods

2.1. Materials

In our study, we employed a variety of materials sourced from reputable suppliers. High molecular weight Chitosan, with a molecular weight ranging from 310,000 to 375,000 Daltons, served as our primary biopolymer, and it was procured from Sigma-Aldrich in the United States. Additional materials included methylene blue (MB), activated charcoal, and sodium chloride, all obtained from the same reliable source, Sigma-Aldrich. To facilitate the crosslinking of Chitosan, we utilized epichlorohydrin as a crosslinking agent, which was acquired from Fluka Analytical in Germany. It's worth noting that all chemicals were utilized without any further purification to maintain consistency in our experiments. Furthermore, to ensure the purity and reliability of our results, we conducted all experiments using double distilled water as the solvent.

2.2. Synthesis of the chitosan-activated charcoal composite

The synthesis of the chitosan-activated charcoal adsorptive composite began with the dissolution of 5 g of chitosan powder in a 500 mL solution of 2% acetic acid. This dissolution step, which took place over the course of 60 minutes under continuous stirring, aimed to ensure the complete integration of chitosan into the acetic acid medium. Following the successful dissolution of chitosan, 1 g of activated charcoal was meticulously added in small portions to the chitosan-acetic acid solution, while gentle stirring was sustained for an additional 30 minutes. Subsequently, a drop-by-drop addition of an epichlorohydrin solution commenced, with the temperature maintained at 70°C, and slow stirring continued for 1 hours to facilitate the crucial crosslinking process. The resultant white precipitate, formed as a result of the chemical interaction, underwent thorough washing with distilled water to eliminate impurities and unreacted components. Subsequent to the washing, the composite was dried overnight at 50°C in a hot air oven to remove residual moisture. Prior to its utilization in adsorption experiments, the composite underwent a final preparation step involving crushing using a pestle and mortar, followed by sieving through a 150-micron mesh to ensure uniformity and eliminate oversized particles, thereby rendering it suitable for use in the intended adsorption studies. The preparation methods of crosslinking Chitosan-activated charcoal adsorptive composite material were shown in Figure 1.

Preprints (www.preprints.org) | NOT PEER-REVIEWED | Posted: 5 October 2023 doi:10.20944/preprints202310.0272.v1

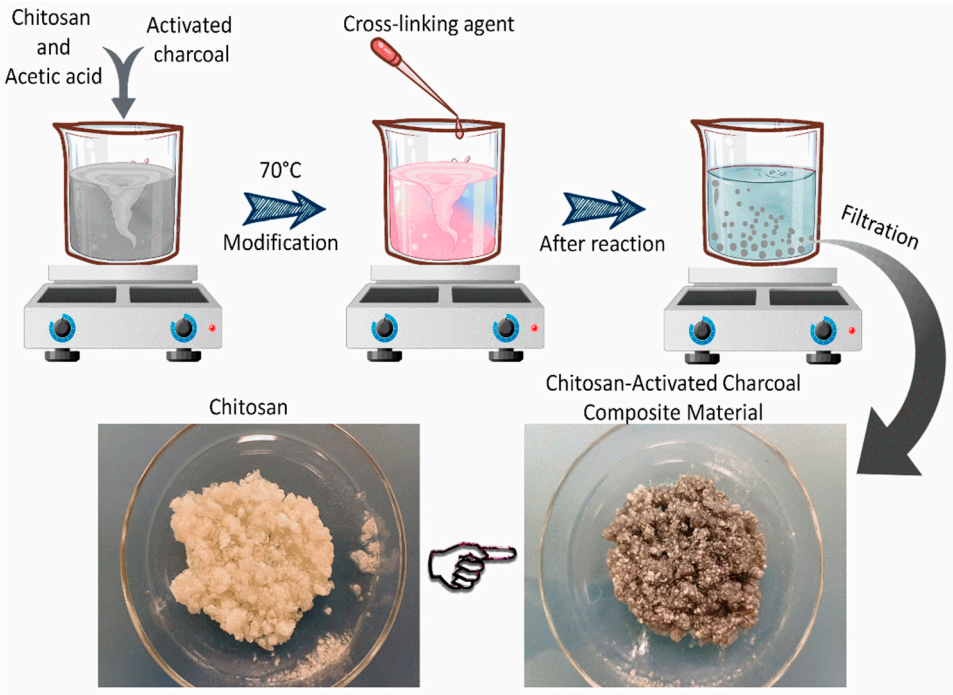

Figure 1. Schematic representation of the preparation of crosslinking Chitosan-activated charcoal adsorptive composite material.

2.3. Characterizations of material

The comprehensive characterization of the synthesized materials played a pivotal role in this study. After the synthesis process and subsequent drying, a multi-faceted approach was employed to elucidate the key properties and composition of the materials.

To gain insights into the surface elemental compositions and to identify functional groups present in both Chitosan and the Chitosan-Activated Charcoal composite material, Fourier transform infrared (FTIR) spectroscopy was conducted. The FTIR analysis was performed using a Vertex 80 spectrometer from Bruker in the United Kingdom. Further exploration of the surface elemental compositions and chemical states of both Chitosan and the Chitosan-Activated Charcoal composite material was conducted using X-ray photoelectron spectroscopy (XPS). The XPS spectrometer utilized for this purpose was the JEOL JPS-9030 model from Japan. Operating at 10 mA and 12 kV with a Mg Kα X-ray source, XPS provided valuable insights into the chemical nature of the materials' surfaces, facilitating a deeper understanding of their molecular composition and bonding configurations.

The thermal and oxidative stability of the membrane were assessed using a thermogravimetric analyzer (TGA) from Mettler Toledo, Austria. For this analysis, synthesized composite material sample weighing 10 mg was placed in a ceramic pan and subjected to examination under a nitrogen atmosphere at a constant flow rate of 40 mL/min. The heating rate was set at 20°C/min, ranging from 50 to 700°C. This TGA analysis offered valuable information regarding the synthesized composite material's response to temperature changes and its oxidative stability, which are key factors in determining its suitability for specific applications. Bottom of Form

2.4. Batch adsorption experiments

The removal of MB dye from aqueous solutions was systematically investigated through batch adsorption experiments. A 50 mL plastic-stoppered round-bottle, equipped with a thermostatic shaker operating at a constant speed of 150 rpm, served as the experimental setup. To maintain consistency, the initial MB dye concentration was set at 25 mg/L, except when exploring concentration effects. A total solution volume of 25 mL was treated in each experiment. The pH of the solution was adjusted using 0.1 N HCl and 0.1 N H_2SO_4 solutions. Several key process parameters,

Preprints (www.preprints.org) | NOT PEER-REVIEWED | Posted: 5 October 2023 doi:10.20944/preprints202310.0272.v1

including solution pH within the range of 3 to 9, adsorbent dosage spanning from 0.1 g to 0.8 g/25 mL, and initial dye concentrations varying from 10 to 200 mg/L, were systematically examined to understand their impact on MB dye removal. Following each experiment, the dye solutions underwent filtration using Whatman filter paper, and the clear filtrate was analyzed for MB dye concentration. The residual MB dye concentration was determined spectrophotometrically using a UV–visible spectrophotometer (Agilent Technologies, Cary 60 UV–Vis) at the λmax of 665 nm. To ensure the reliability of the results, experimental replicates were conducted at least twice to obtain an average value, which is subsequently reported. The removal percentage of MB dye was calculated according to the flowing equation:

$$Dye\ removal\ (\%) = \frac{C_0 - C_f}{C_0} \times 100$$

where, C_0 and C_f are initial and final concentration of dye.

3. Results and Discussion

3.1. X-ray Photoelectron Spectroscopy (XPS) analysis of synthesised material

XPS is a powerful analytical tool used to investigate the surface composition and chemical functionalities of materials. In this study, XPS analysis was employed to characterize the surface properties of two materials: chitosan and a cross-linked chitosan-activated charcoal composite material. The XPS survey spectra for both materials are presented in Figures 2 and 3, allowing us to gain insights into their elemental composition. Figure 2 illustrates the XPS survey spectrum of chitosan. In this spectrum, we observe strong peaks at binding energies of 285 eV, 400 eV, and 532 eV, corresponding to the elements carbon (C), nitrogen (N), and oxygen (O), respectively. These peaks are indicative of the elemental composition present on the surface of the chitosan material. The presence of C, N, and O is consistent with what is expected for chitosan. Figure 3 displays the XPS survey spectrum of the cross-linked chitosan-activated charcoal composite material. Similar to chitosan, this spectrum exhibits prominent peaks at 285 eV, 400 eV, and 532 eV, signifying the presence of C, N, and O elements on the material's surface.

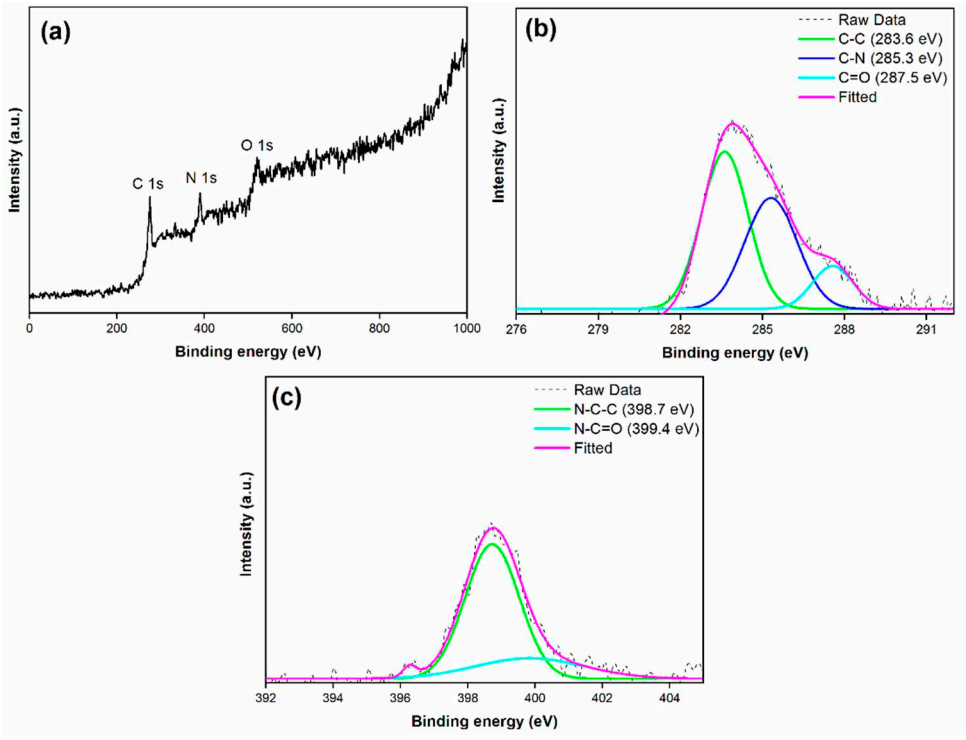

Figure 2. Surface Chemical Characterization of the Chitosan Material. (a) XPS Survey Spectrum. High-resolution XPS Spectra and Peak Deconvolution of (b) C (1s) Spectra, and (c) N (1s) Spectra.

Preprints (www.preprints.org) | NOT PEER-REVIEWED | Posted: 5 October 2023 doi:10.20944/preprints202310.0272.v1

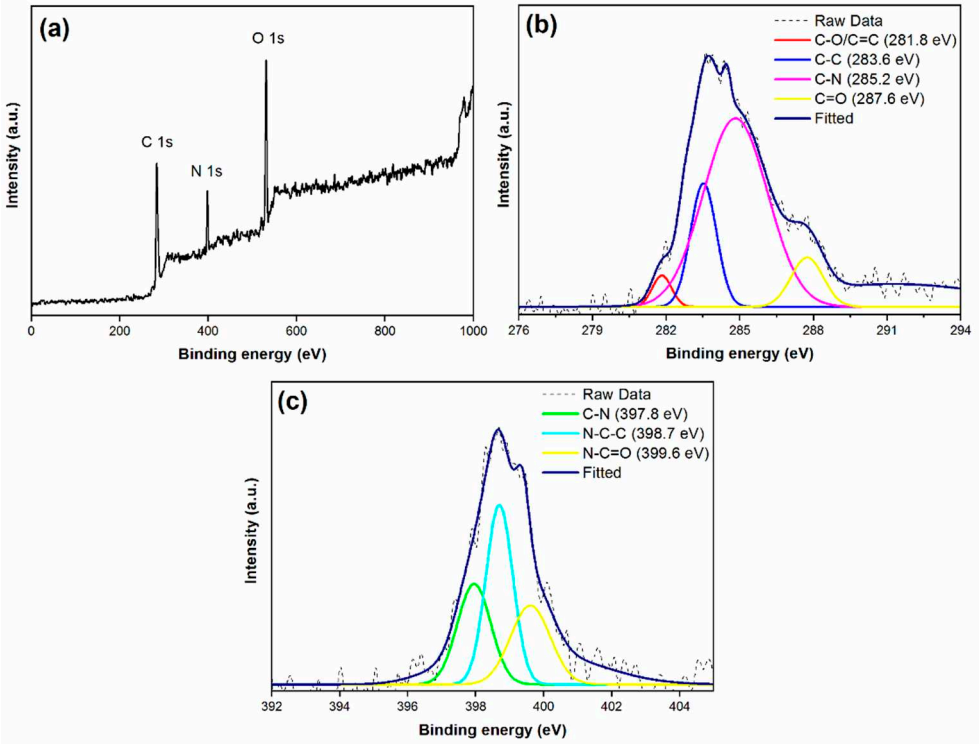

Figure 3. Surface Chemical Characterization of the Chitosan-Activated Charcoal composite material. (a) XPS Survey Spectrum. High-resolution XPS Spectra and Peak deconvolution of (b) C (1s) Spectra, and (c) N (1s) Spectra.

This observation confirms that the composite material retains the elemental composition of chitosan while incorporating activated charcoal. To delve deeper into the surface chemistry and identify specific functional groups on the cross-linked chitosan-activated charcoal composite material, high-resolution XPS spectra were analyzed, as demonstrated in Figure 3b and Figure 3c. Figure 3b shows the high-resolution C (1s) spectrum of the composite material. In this spectrum, four distinct peaks are discernible. The main peak at 281.8 eV is attributed to C−O or C=C bonds, suggesting the presence of oxygen-containing functional groups. An intermediate peak at 283.6 eV corresponds to C−C bonds, indicating the existence of carbon-carbon linkages. The peak at 285.2 eV is associated with C−N bonds, indicating the presence of nitrogen-containing groups. Lastly, the peak at 287.6 eV is attributed to the C=O bond, indicating the presence of carbonyl groups on the surface of the composite material. Figure 3c presents the N (1s) core-level spectrum of the composite material, which also exhibits four distinct peaks. The peak at 397.9 eV can be assigned to the C−N bond, confirming the presence of nitrogen atoms involved in carbon-nitrogen interactions. The peak at 398.7 eV corresponds to the N−C−C bond, indicating the presence of alkylamine groups. Interestingly, there is a minor typographical error in the text mentioning "4399.6 eV." It should read "399.6 eV." This peak is likely attributed to the N−C=O bond, suggesting the presence of amide or imine groups containing oxygen. The presence of specific functional groups can influence the material's reactivity and adsorption capabilities, making it a valuable candidate for various environmental and industrial applications.

3.2. FTIR analysis of synthesised material

The FTIR analysis was employed to characterize the functional groups within both the chitosan and the chitosan-activated charcoal composite material. As depicted in Figure 4, the infrared spectrum of the composite material reveals several significant absorption bands. Notably, a strong band at approximately 3283 cm^{-1} can be attributed to N-H and O-H stretching vibrations, signifying the presence of intramolecular hydrogen bonds within the material. Additionally, two absorption

Preprints (www.preprints.org) | NOT PEER-REVIEWED | Posted: 5 October 2023 doi:10.20944/preprints202310.0272.v1

bands at approximately 2921 and 2868 cm^{-1} are indicative of C-H symmetric and asymmetric stretching, respectively. These particular bands are commonly associated with polysaccharides and are consistent with similar spectra of other polysaccharide materials. Further examination of the composite material's spectrum confirms the presence of residual N-acetyl groups, as evidenced by the absorption band at approximately 1646 cm^{-1}, corresponding to the C=O stretching of amide I. Additionally, a minor band at 1547 cm^{-1}, which corresponds to the N-H bending of amide II, is observed. This band is characteristic of N-acetyl groups, although it may be partially overlapped by other spectral features. Another noteworthy feature in the spectrum is the absorption band at 1596 cm^{-1}, representing the N-H bending of primary amines. Finally, the absorption band at 1219 cm^{-1} can be attributed to the asymmetric stretching of the C-O-C bridge, providing insights into the material's structural composition. Two additional bands at 1076 and 1028 cm^{-1} correspond to C-O stretching vibrations, further contributing to our understanding of the functional groups and chemical bonds present within the chitosan-activated charcoal composite material. These FTIR results offer valuable information regarding the molecular composition and structural characteristics of the composite, facilitating a comprehensive analysis of its potential applications and properties.

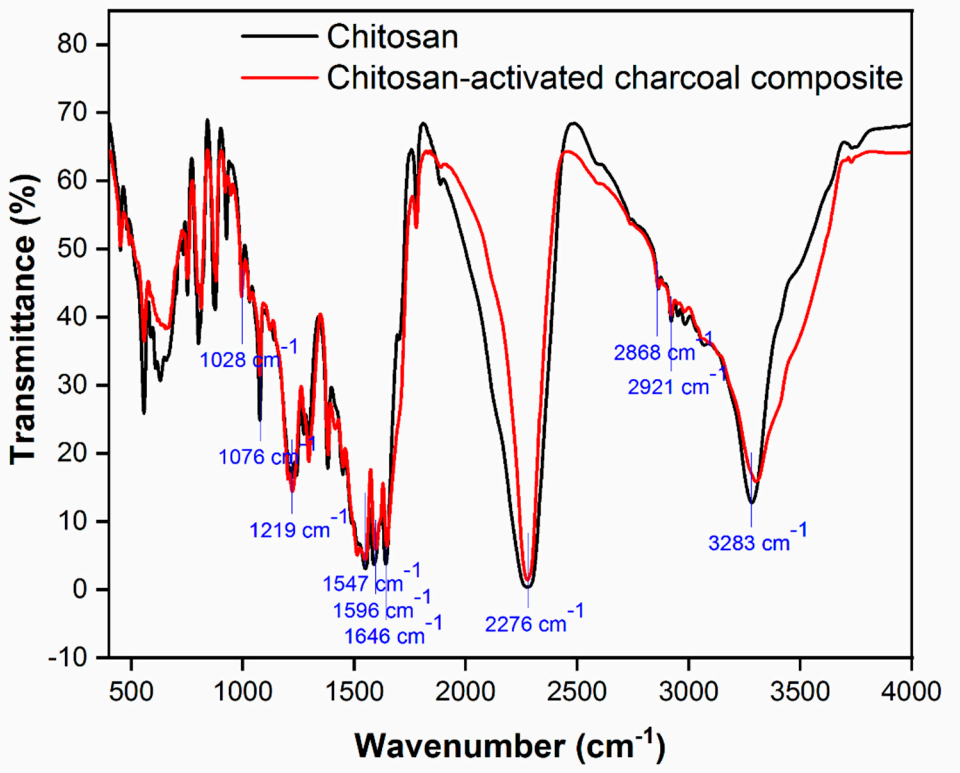

Figure 4. FTIR spectra of synthesized materials depicting the molecular composition and functional groups within the Chitosan-Activated Charcoal composite material.

3.3. Zeta-potential analysis of synthesised material

The zeta potential analysis results provide valuable insights into the surface charge characteristics of Chitosan and its potential as a platform for adsorbing MB dye after cross-linking with activated charcoal. As depicted in Figure 5, pure Chitosan displayed a zeta potential of -9 mV, indicating a mild negative charge due to protonated amine groups ($-NH_2$) on its polymer chains. While this suggests some degree of electrostatic repulsion among Chitosan particles, the relatively low magnitude may make it susceptible to aggregation, limiting its adsorption capacity for MB dye. However, after cross-linking with activated charcoal, the chitosan-activated charcoal composite material exhibited a substantial increase in zeta potential, measuring at -26 mV. This significant enhancement in negative zeta potential is promising for adsorption applications. The introduction of activated charcoal, known for its negatively charged functional groups, likely played a crucial role in

Preprints (www.preprints.org) | NOT PEER-REVIEWED | Posted: 5 October 2023 doi:10.20944/preprints202310.0272.v1

this increase. The higher negative charge implies improved electrostatic repulsion among particles in the composite material, enhancing its stability and potential as an efficient adsorbent for MB dye. This substantial zeta potential increase suggests that the chitosan-activated charcoal composite material could be a highly effective adsorbent for MB dye removal from aqueous solutions. Its enhanced surface charge and improved stability make it well-suited for applications in wastewater treatment and environmental remediation, where efficient dye removal is crucial. Further studies to characterize its adsorption capacity would be valuable for confirming its suitability in practical dye removal processes.

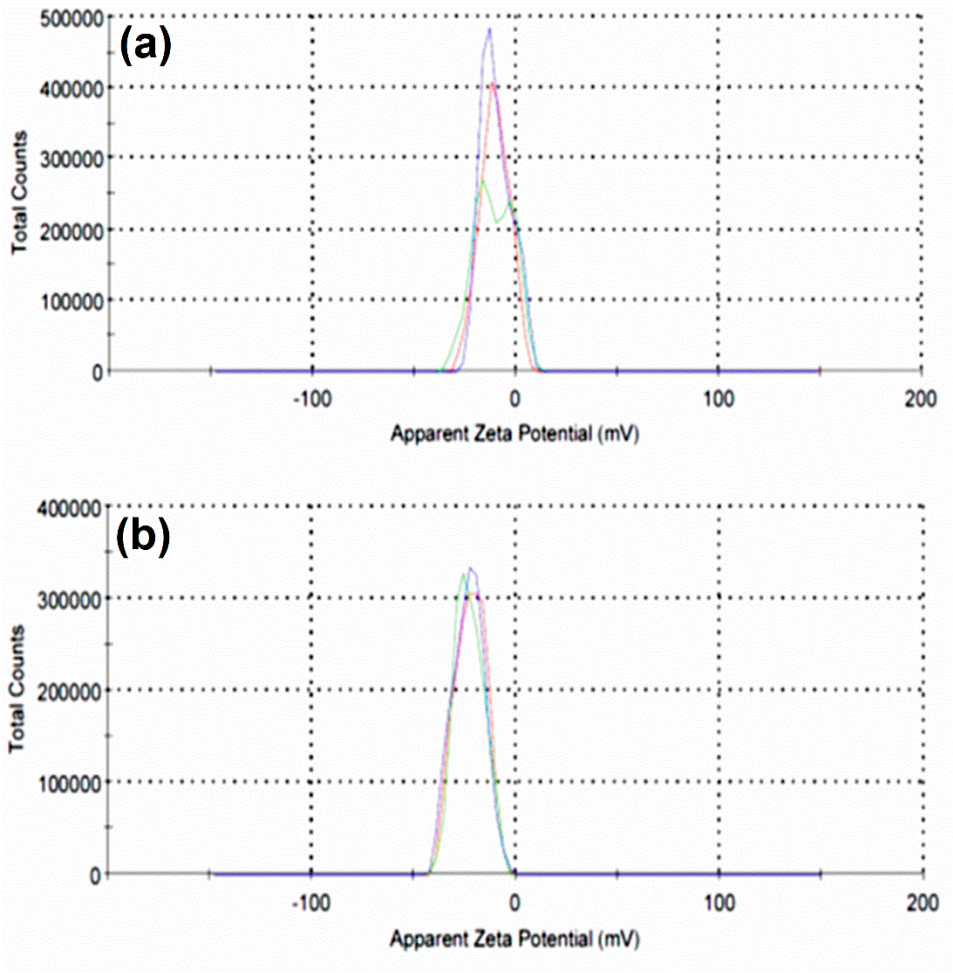

Figure 5. zeta potential distribution synthesised materials (a) chitosan and (b) chitosan-activated charcoal composite materials.

3.4. Thermogravimetric analysis (TGA) of synthesised materials

TGA serves as a valuable analytical tool for assessing the thermal characteristics, composition, and purity of materials. In our study, we utilized TGA to investigate the impact of cross-linked activated charcoal on the thermal stability of chitosan, depicted in Figure 6. The results of the TGA analysis, along with their corresponding derivative thermogravimetry (DTG) plots, are presented in Figure 6 for both chitosan and the cross-linked chitosan-activated charcoal composite material. In Figure 6a, the TGA curve for chitosan reveals a distinct weight loss pattern, indicating the onset of polymer chain decomposition. This decomposition process commences at approximately 156°C and extends up to 316°C. These temperature ranges mark the significant thermal degradation zones for pure chitosan. Conversely, Figure 6b depicts the TGA curve for the chitosan-activated charcoal composite material. Here, we observe a noticeable shift in the thermal stability profile compared to pure chitosan. The composite material exhibits thermal degradation beginning at approximately 223°C and continuing until around 323°C. This extended thermal stability range suggests that the

Preprints (www.preprints.org) | NOT PEER-REVIEWED | Posted: 5 October 2023 doi:10.20944/preprints202310.0272.v1

presence of activated charcoal has a substantial influence on enhancing the thermal stability of the chitosan matrix. These results emphasize the beneficial impact of activated charcoal cross-linking on the enhanced thermal stability of the composite material compared to pure chitosan.

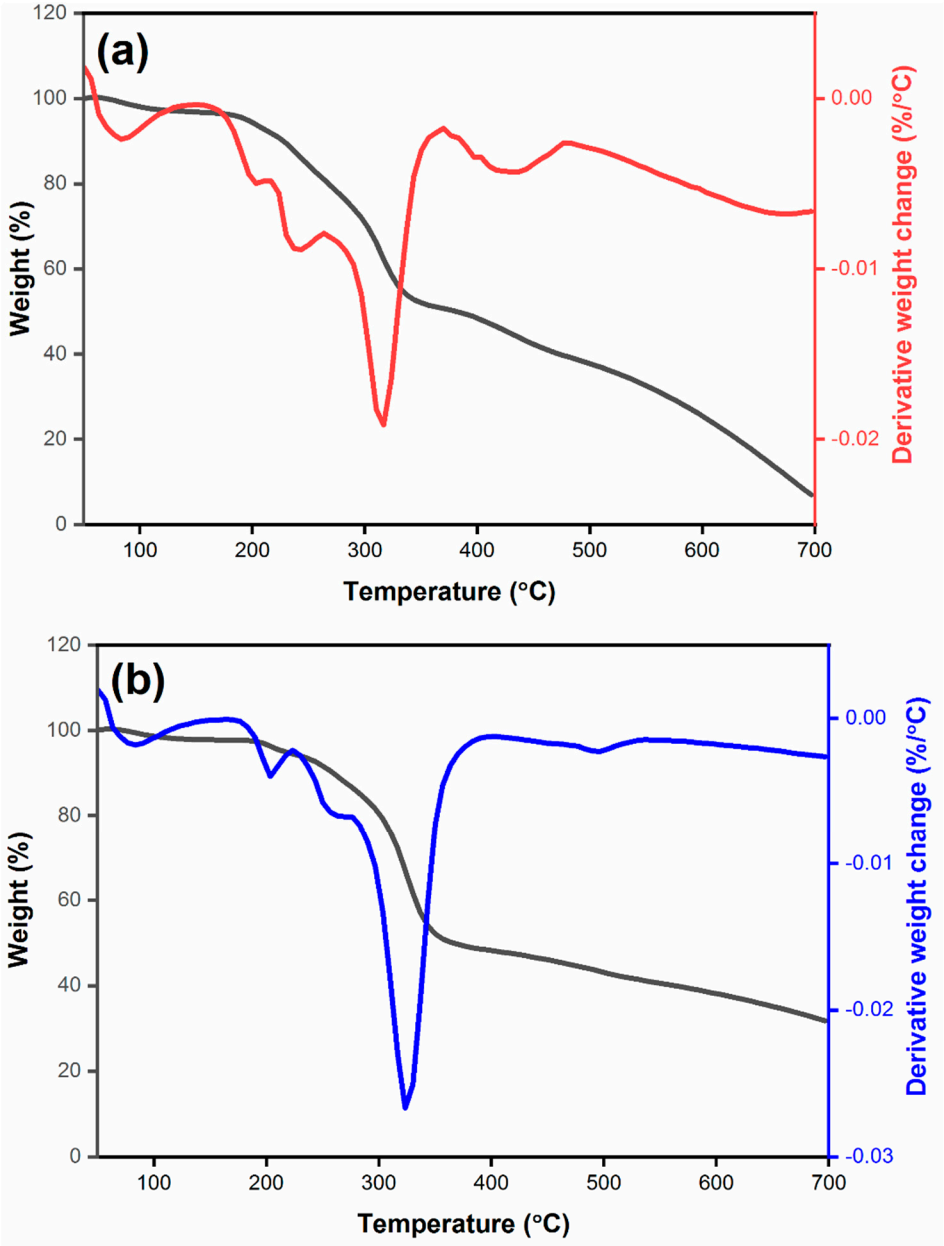

Figure 6. Thermogravimetric analysis of synthesized materials, including (a) chitosan and (b) chitosan-activated charcoal composite materials.

3.5. Effect of adsorbent dosage on the adsorption capacity

The impact of adsorbent dosage on the removal of MB dye from aqueous solutions was thoroughly investigated in this study. Various dosages of the adsorbent, ranging from 0.1 g to 0.8 g/25 mL of the solution, were examined while keeping other parameters constant, including an initial MB dye concentration of 25 mg/L, a pH level of 7, a contact time of 240 minutes, and a temperature of 25°C. The results of this investigation are presented in Figure 7, which illustrates the relationship between adsorbent dosage and the percentage removal of MB dye. As seen in Figure 7, an intriguing trend emerges with changes in the adsorbent dosage. It becomes evident that the removal efficiency of MB dye increases as the dosage of the adsorbent is augmented. This observed phenomenon can be attributed to several factors. Firstly, the increase in the adsorbent dosage provides a larger surface area available for interaction with MB dye molecules. Consequently, a greater number of active

Preprints (www.preprints.org) | NOT PEER-REVIEWED | Posted: 5 October 2023 doi:10.20944/preprints202310.0272.v1

adsorption sites become accessible for the dye molecules to attach to, enhancing the overall adsorption capacity. Figure 6 further reveals that the adsorption of the MB dye exhibits a rapid increase up to an adsorbent dosage of 0.4 g/25 mL. Beyond this point, there is only a marginal increase in adsorption efficiency with further increments in adsorbent dosage. This observation indicates that there is an optimal dosage at which the adsorption process achieves maximum efficiency, and beyond this point, additional adsorbent does not significantly contribute to increased dye removal. Based on the findings presented above, it is evident that the optimum adsorbent dosage for achieving the maximum removal efficiency of MB dye from wastewater is 0.4 g/25 mL. This dosage strikes a balance between providing an ample surface area and active sites for adsorption while avoiding excess adsorbent that may not substantially improve the removal process. Therefore, 0.4 g/25 mL is the recommended dosage for effective MB dye removal in this study.

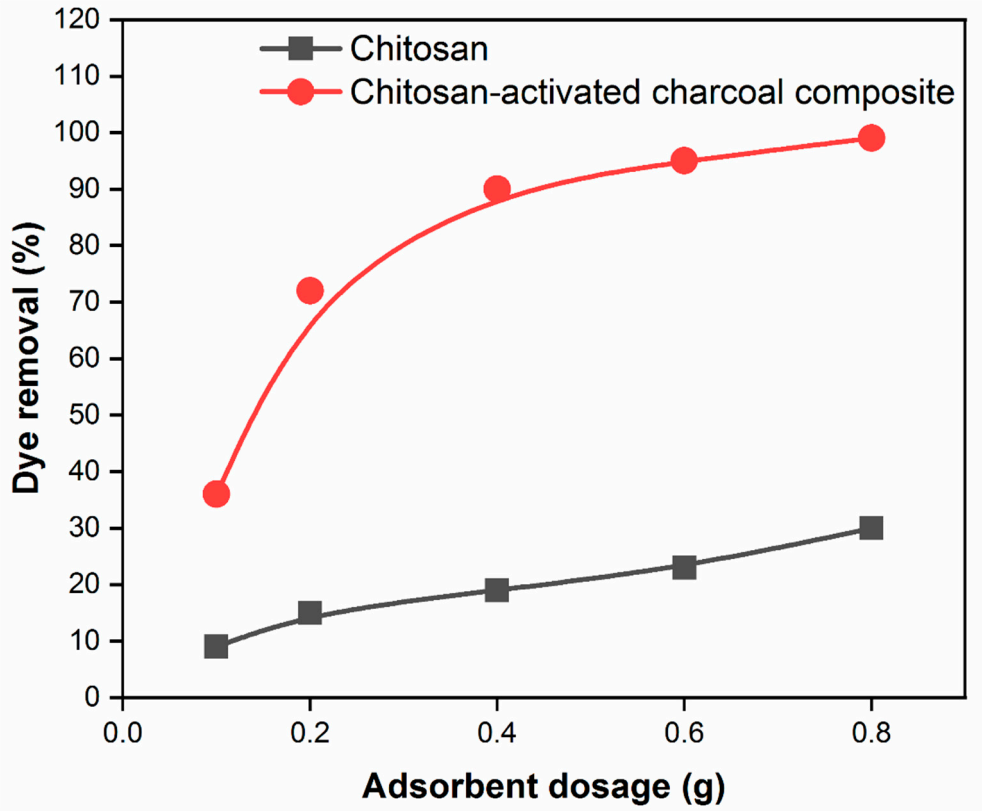

Figure 7. Effect of adsorbent dosage (0.1 g to 0.8 g/25 mL) on the removal of MB dye.

3.6. The effect of pH on the adsorption capacity

The pH of a solution is a critical factor affecting the efficiency of adsorption processes, particularly when employing chitosan and chitosan-activated charcoal composite materials for the removal of dyes from aqueous systems. To gain a comprehensive understanding of this effect, we conducted a series of experiments covering a pH range from 3 to 9, maintaining a consistent adsorbent dosage of 0.6 g/25 mL, a temperature of 25 °C, an initial MB dye concentration of 25 mg/L, and a contact time of 240 minutes. The results of these experiments are presented in Figure 8. Figure 8 provides a compelling visualization of the pH-dependent trends in MB dye removal when using the composite material. It is evident that as the pH level increased from 3 to 9, the removal efficiency of MB dye experienced a notable decrease. Remarkably, the highest removal rate, reaching 95%, was attained at a pH of 3 after 240 minutes of contact time, outperforming the performance of chitosan as an adsorbent under the same conditions. The enhanced removal of MB dye at lower pH values can be attributed to the unique characteristics of the chitosan-activated charcoal composite material. Specifically, under acidic conditions (pH 3), this composite material becomes positively charged. This positive charge results from the interaction between the acidic pH and the functional groups on the surface of the material, creating an electrostatic attraction between the cationic MB dye molecules and

Preprints (www.preprints.org) | NOT PEER-REVIEWED | Posted: 5 October 2023 doi:10.20944/preprints202310.0272.v1

the positively charged composite material. This attractive force facilitates the adsorption of MB dye onto the composite, leading to significantly improved adsorption efficiency at pH 3. Conversely, the decrease in MB dye removal percentage observed at higher pH values (pH 9) can be attributed to a different set of interactions. At higher pH levels, the aqueous solution contains an excess of hydroxyl ions (OH^-), which introduces competition for the available adsorption sites on the surface of the adsorbent material. This competition arises because the anionic groups present in the MB dye molecules and the hydroxyl ions both seek to occupy the adsorption sites. Consequently, the adsorption efficiency of the dye decreases as the OH^- ions interfere with the binding of MB dye to the adsorbent surface. These findings underscore the importance of pH control when designing efficient adsorption processes for dye removal from aqueous systems using composite materials.

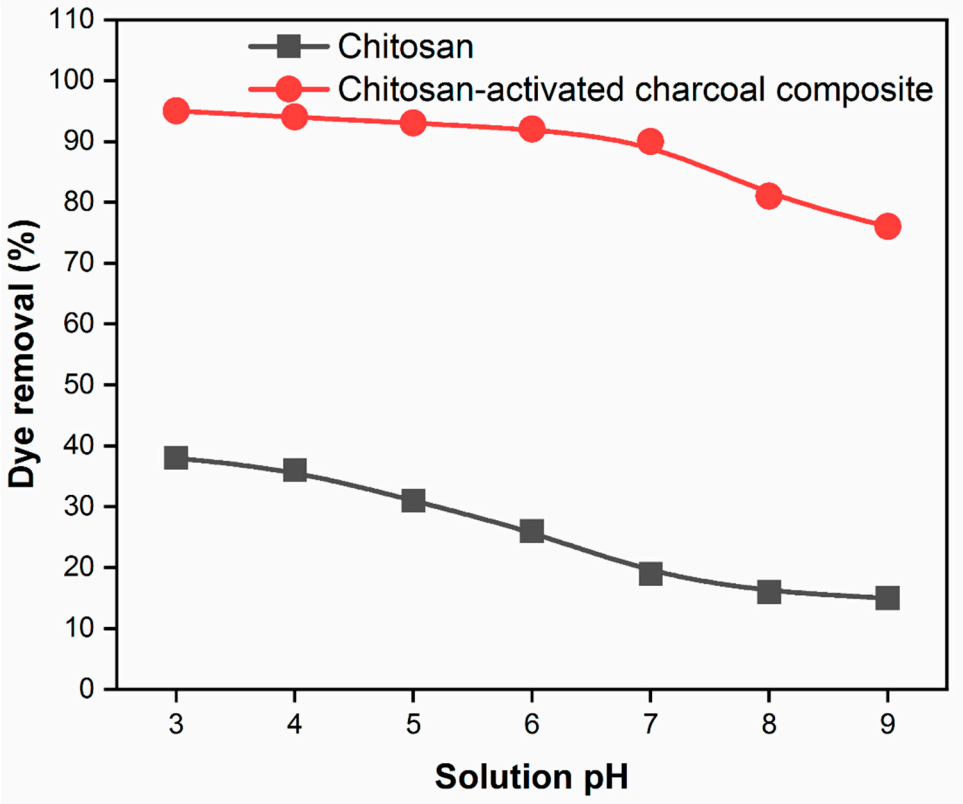

Figure 8. Effect of pH (3 to 9) on dye removal.

3.7. Effect of dye concentration on the adsorption capacity

The influence of MB dye concentration on the adsorption capacity was a critical aspect of our study. To explore this, we conducted experiments across a range of MB dye concentrations, specifically at levels of 10, 25, 50, 100, and 200 mg/L. Throughout these experiments, we maintained a consistent adsorbent dosage of 0.4 g/25 mL, a temperature of 25°C, and a pH level of 7. The outcomes of these experiments are depicted in Figure 9, which graphically represents the relationship between MB dye concentration and the removal efficiency. The results obtained clearly demonstrate a significant and noteworthy trend. The removal percentage of MB dye exhibited an inverse relationship with its concentration in the solution. In other words, as the MB dye concentration increased, the removal efficiency decreased. For chitosan, the removal efficiency decreased from 25% at a lower MB concentration of 10 mg/L to 5% when the concentration was increased to 200 mg/L. This trend suggests that chitosan's adsorption capacity is adversely affected by higher concentrations of MB dye. Conversely, the chitosan-activated charcoal composite material displayed a different behavior. It exhibited a removal percentage ranging from 95% at a lower MB concentration of 10 mg/L to 81% when the concentration was raised to 200 mg/L for the cross-linked activated charcoal with chitosan composite. This indicates a relatively high and consistent adsorption capacity, even at higher MB dye concentrations, compared to chitosan alone. The observed decrease in removal efficiency at

Preprints (www.preprints.org) | NOT PEER-REVIEWED | Posted: 5 October 2023 doi:10.20944/preprints202310.0272.v1

higher dye concentrations can be attributed to the saturation of adsorption sites on the adsorbent surface. As the concentration of MB dye in the solution increases, there is a higher competition for available adsorption sites, leading to a reduced overall adsorption efficiency.

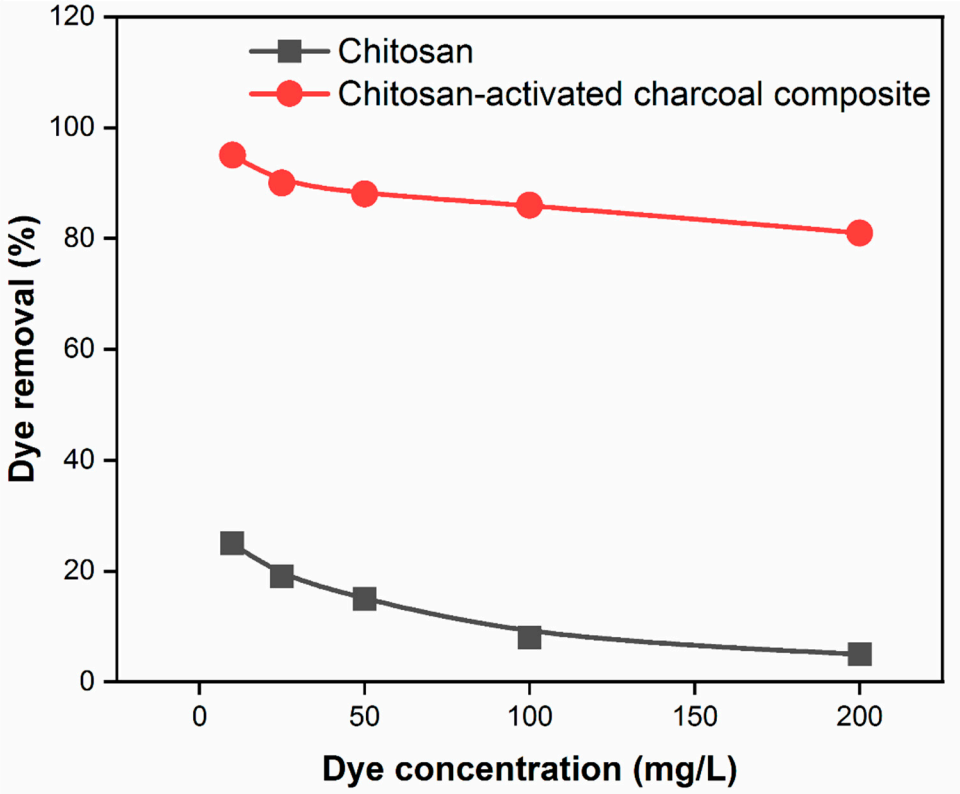

Figure 9. Effect of dye concentration (10-200 mg/L) on the removal of MB dye.

3.8. Effect of reaction time for dye adsorption capacity

The investigation into the effect of reaction time on the adsorption capacity of MB dye was a crucial aspect of our study. To explore this, experiments were conducted over a range of reaction times, extending up to 600 minutes, using both chitosan and the chitosan-activated charcoal composite adsorbent material. These experiments were performed at a constant adsorbent dosage of 0.4 g/25 mL, a temperature of 25°C, and a pH level of 7. The results obtained from these experiments are depicted in Figure 10, which illustrates the relationship between reaction time and the removal efficiency of MB dye. From the data presented in Figure 10, it is evident that the composite adsorbent material exhibited a distinct trend in its response to varying reaction times. Initially, the removal percentage of MB dye increased significantly with time, reaching 95% removal efficiency at 360 minutes of reaction time. Subsequently, the dye adsorption remained constant, with a maximum removal percentage of 99% achieved. This behavior signifies that the composite adsorbent reached its maximum adsorption capacity within the first 360 minutes of the reaction, after which it achieved a state of equilibrium. Beyond this point, further prolonging the reaction time did not lead to a substantial increase in the removal efficiency, indicating that the adsorption sites on the composite material had become saturated. In contrast, the chitosan material displayed a comparatively lower removal percentage across different reaction times. This observation suggests that chitosan reached its adsorption equilibrium at a lower efficiency level compared to the composite material and was less effective in removing MB dye from the solution, regardless of the reaction time. The chitosan-activated charcoal composite material exhibited remarkable efficiency, with a rapid increase in removal percentage up to 360 minutes, followed by a plateau at 99%. This underscores the importance of optimizing reaction times in adsorption processes to achieve maximum pollutant removal. Additionally, the composite material clearly outperformed pure chitosan in terms of MB dye removal, emphasizing its potential as an effective adsorbent for wastewater treatment applications.

Preprints (www.preprints.org) | NOT PEER-REVIEWED | Posted: 5 October 2023 doi:10.20944/preprints202310.0272.v1

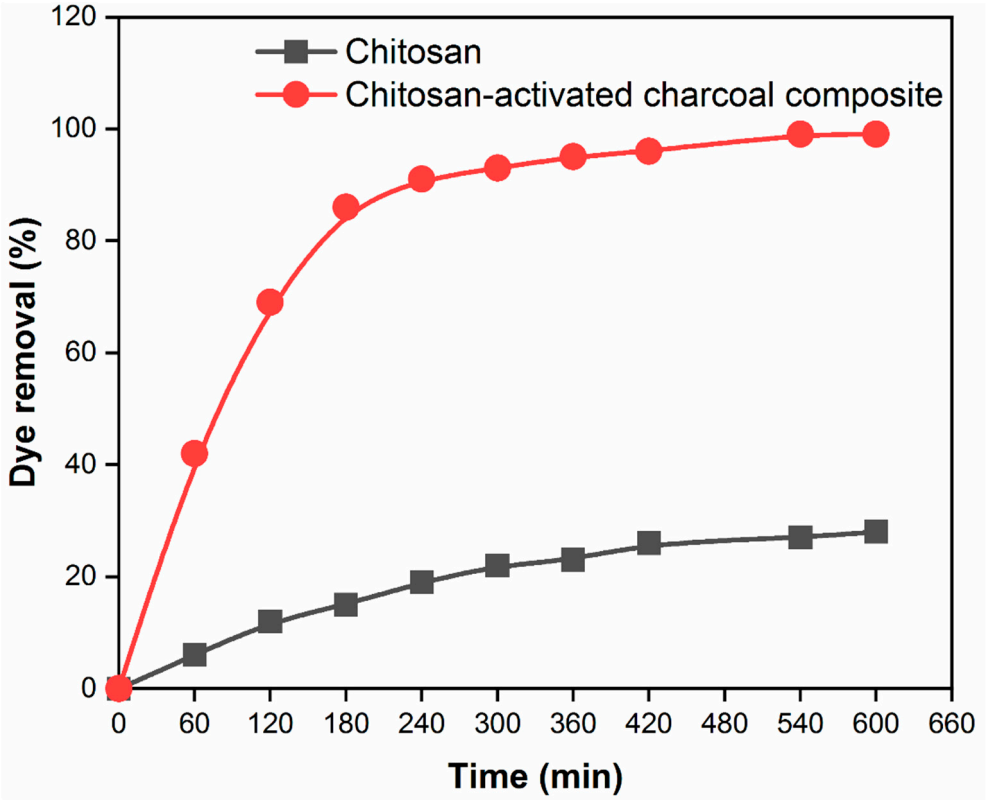

Figure 10. Effect of contact time on the adsorption of MB dye.

4. Conclusions

In conclusion, our research successfully yielded chitosan-activated charcoal composite materials via crosslinking with epichlorohydrin, with the overarching goal of creating a highly effective adsorbent for the removal of MB dye from water. Employing advanced analytical techniques, including FTIR, XPS, and TGA, we comprehensively examined the physical, chemical, and structural attributes of these composites. The XPS analysis unequivocally confirmed that the composite material retains chitosan's elemental composition while incorporating activated charcoal, a pivotal factor in its adsorption capabilities. Additionally, FTIR analysis afforded insights into the functional groups present in both chitosan and the composite, enhancing our understanding of its chemical structure. Of particular note, the zeta potential analysis underscored the augmented surface charge characteristics of the chitosan-activated charcoal composite following cross-linking, which substantially bolstered its adsorption potential. Significantly, TGA analysis revealed a substantial shift in thermal stability compared to pure chitosan, showcasing the vastly improved stability of the composite material. When we delved into the influence of adsorbent dosage, a captivating trend emerged: the removal efficiency of MB dye increased proportionally with higher dosages, culminating at 0.4 g/25 mL, after which additional increments yielded diminishing returns. This pivotal finding highlights the existence of an optimal dosage for maximizing dye removal efficiency. Exploring the pH-dependent trends, we observed the composite's exceptional performance in lower pH conditions, achieving a striking 95% removal rate at pH 3 after 240 minutes of contact time, surpassing the efficacy of chitosan in isolation. This underscores the composite's potential in the effective removal of dyes in acidic environments. Furthermore, our examination of the influence of MB dye concentration unveiled a distinctive behavior in the composite, maintaining high removal percentages across a spectrum of concentrations, ranging from 95% at 10 mg/L to 81% at 200 mg/L. This versatility positions it as a valuable tool for efficient dye removal under diverse circumstances. Lastly, across varying reaction times, the composite adsorbent exhibited a unique pattern, reaching its peak adsorption capacity within the initial 360 minutes before attaining a stable equilibrium with an impressive 99% removal efficiency. In conclusion, our study underscores the considerable promise

of the chitosan-activated charcoal composite material as an adsorbent for MB dye removal from water, offering enhanced efficiency, stability, and adaptability across a range of conditions. Further research and optimization endeavors are warranted to fully harness its potential for addressing water pollution challenges and environmental remediation.

Author Contributions: Conceptualization, A.K.S. and J.A.; methodology, AKS.; validation, J.R. and K.K.K.; formal analysis, J.A.; investigation, A.K.S.; resources, J.A.; data curation, J.R. and K.K.K.; writing—original draft preparation, A.K.S.; writing—review and editing, A.K.S.; J.A.; and K.K.K.; supervision, J.A. and J.R.; funding acquisition, J.A. All authors have read and agreed to the published version of the manuscript.

Funding: Not applicable.

Data Availability Statement: Not applicable.

Conflicts of Interest: The authors declare no conflict of interest.

References

1. Zhang, N.; Jiang, B.; Zhang, L.; Huang, Z.; Sun, Y.; Zong, Y.; Zhang, H. Low-pressure electroneutral loose nanofiltration membranes with polyphenol-inspired coatings for effective dye/divalent salt separation. *Chem. Eng. J.* **2019**, *359*, 1442–1452.
2. Dawood, S.; Sen, T.K.; Phan, C. Adsorption removal of Methylene Blue (MB) dye from aqueous solution by bio-char prepared from Eucalyptus sheathiana bark: kinetic, equilibrium, mechanism, thermodynamic and process design. *Desalin. Water Treat.* **2016**, *57*, 28964–28980.
3. Harrou, A.; Gharibi, E.; Nasri, H.; El Ouahabi, M. Thermodynamics and kinetics of the removal of methylene blue from aqueous solution by raw kaolin. *SN Appl. Sci.* **2020**, *2*, 1–11.
4. Rajoriya, S.; Saharan, V.K.; Pundir, A.S.; Nigam, M.; Roy, K. Adsorption of methyl red dye from aqueous solution onto eggshell waste material: Kinetics, isotherms and thermodynamic studies. *Curr. Res. Green Sustain. Chem.* **2021**, *4*, 100180.
5. Aragaw, T.A.; Alene, A.N. A comparative study of acidic, basic, and reactive dyes adsorption from aqueous solution onto kaolin adsorbent: Effect of operating parameters, isotherms, kinetics, and thermodynamics. *Emerg. Contam.* **2022**, *8*, 59–74.
6. Gürses, A.; Hassani, A.; Kranşan, M.; Açşl, Ö.; Karaca, S. Removal of methylene blue from aqueous solution using by untreated lignite as potential low-cost adsorbent: Kinetic, thermodynamic and equilibrium approach. *J. Water Process Eng.* **2014**, *2*, 10–21.
7. Brahma, D.; Saikia, H. Synthesis of ZrO2/MgAl-LDH composites and evaluation of its isotherm, kinetics and thermodynamic properties in the adsorption of congo red dye. *Chem. Thermodyn. Therm. Anal.* **2022**, *7*, 100067.
8. Maruthapandi, M.; Kumar, V.B.; Luong, J.H.T.; Gedanken, A. Kinetics, Isotherm, and Thermodynamic Studies of Methylene Blue Adsorption on Polyaniline and Polypyrrole Macro-Nanoparticles Synthesized by C-Dot-Initiated Polymerization. *ACS Omega* **2018**, *3*, 7196–7203.
9. Salunkhe, B.; Schuman, T.P. Super-Adsorbent Hydrogels for Removal of Methylene Blue from Aqueous Solution: Dye Adsorption Isotherms, Kinetics, and Thermodynamic Properties. *Macromol* **2021**, *1*, 256–275.
10. Tan, Y.; Sun, Z.; Meng, H.; Han, Y.; Wu, J.; Xu, J.; Xu, Y.; Zhang, X. A new MOFs/polymer hybrid membrane: MIL-68(Al)/PVDF, fabrication and application in high-efficient removal of p-nitrophenol and methylene blue. *Sep. Purif. Technol.* **2019**, *215*, 217–226.
11. Rafatullah, M.; Sulaiman, O.; Hashim, R.; Ahmad, A. Adsorption of methylene blue on low-cost adsorbents: A review. *J. Hazard. Mater.* **2010**, *177*, 70–80.
12. Badrinezhad, L.; Ghasemi, S.; Azizian-Kalandaragh, Y.; Nematollahzadeh, A. Preparation and characterization of polysulfone/graphene oxide nanocomposite membranes for the separation of methylene blue from water. *Polym. Bull.* **2018**, *75*, 469–484.
13. Alam, J.; Shukla, A.K.; Ansari, M.A.; Abdulraqeb, F.; Ali, A.; Alhoshan, M. Dye Separation and Antibacterial Activities of Polyaniline Thin Film-Coated Poly (phenyl sulfone) Membranes. *Membranes (Basel).* **2021**, *11*, 25–40.
14. Khademian, E.; Salehi, E.; Sanaeepur, H.; Galiano, F.; Figoli, A. A systematic review on carbohydrate biopolymers for adsorptive remediation of copper ions from aqueous environments-part A: Classification and modification strategies. *Sci. Total Environ.* **2020**, *738*, 139829.

15. Rashed, M.N. Adsorption Technique for the Removal of Organic Pollutants from Water and Wastewater. In; Rashed, M.N., Ed.; IntechOpen: Rijeka, 2013; p. Ch. 7.
16. Quesada, H.B.; Baptista, A.T.A.; Cusioli, L.F.; Seibert, D.; de Oliveira Bezerra, C.; Bergamasco, R. Surface water pollution by pharmaceuticals and an alternative of removal by low-cost adsorbents: A review. *Chemosphere* **2019**, *222*, 766–780.
17. Ohale, P.E.; Igwegbe, C.A.; Iwuozor, K.O.; Emenike, E.C.; Obi, C.C.; Białowiec, A. A review of the adsorption method for norfloxacin reduction from aqueous media. *MethodsX* **2023**, *10*, 102180.
18. Gan, Y.X. Activated Carbon from Biomass Sustainable Sources. *C* **2021**, *7*, 39.
19. Zhao, X.; Huang, C.; Zhang, S.; Wang, C. Cellulose Acetate/Activated Carbon Composite Membrane with Effective Dye Adsorption Performance. *J. Macromol. Sci. Part B Phys.* **2019**, *58*, 909–920.
20. Elmaghraby, N.A.; Omer, A.M.; Kenawy, E.R.; Gaber, M.; Ragab, S.; Nemr, A. El Composite nanofiber formation using a mixture of cellulose acetate and activated carbon for oil spill treatment. *Environ. Sci. Pollut. Res.* **2023**, *30*, 38683–38699.
21. Mahor, A.; Singh, P.P.; Bharadwaj, P.; Sharma, N.; Yadav, S.; Rosenholm, J.M.; Bansal, K.K. Carbon-Based Nanomaterials for Delivery of Biologicals and Therapeutics: A Cutting-Edge Technology. *C* **2021**, *7*, 19.
22. Rendón-Villalobos, R.; Ortíz-Sánchez, A.; Sánchez, E.T.; Flores-Huicochea, E. The Role of Biopolymers in Obtaining Environmentally Friendly Materials. In; Poletto, M., Ed.; IntechOpen: Rijeka, 2016; p. Ch. 8 ISBN 978-953-51-2794-9.
23. S, H.; U Chandran, G.; P R, J.; Sambhudevan, S. Biomedical Applications of Chitin BT - Handbook of Biopolymers. In; Thomas, S., AR, A., Jose Chirayil, C., Thomas, B., Eds.; Springer Nature Singapore: Singapore, 2022; pp. 1–28 ISBN 978-981-16-6603-2.
24. Jiménez-Gómez, C.P.; Cecilia, J.A. Chitosan: A Natural Biopolymer with a Wide and Varied Range of Applications. *Molecules* **2020**, *25*.
25. Piekarska, K.; Sikora, M.; Owczarek, M.; Jóźwik-Pruska, J.; Wiśniewska-Wrona, M. Chitin and Chitosan as Polymers of the Future—Obtaining, Modification, Life Cycle Assessment and Main Directions of Application. *Polymers (Basel).* **2023**, *15*.
26. Croisier, F.; Jérôme, C. Chitosan-based biomaterials for tissue engineering. *Eur. Polym. J.* **2013**, *49*, 780–792.
27. Brasselet, C.; Pierre, G.; Dubessay, P.; Dols-Lafargue, M.; Coulon, J.; Maupeu, J.; Vallet-Courbin, A.; de Baynast, H.; Doco, T.; Michaud, P.; et al. Modification of chitosan for the generation of functional derivatives. *Appl. Sci.* **2019**, *9*.
28. Harugade, A.; Sherje, A.P.; Pethe, A. Chitosan: A review on properties, biological activities and recent progress in biomedical applications. *React. Funct. Polym.* **2023**, *191*, 105634.
29. Cheung, R.C.F.; Ng, T.B.; Wong, J.H.; Chan, W.Y. *Chitosan: An update on potential biomedical and pharmaceutical applications*; 2015; Vol. 13; ISBN 8523943803.
30. Grzybek, P.; Jakubski, Ł.; Dudek, G. Neat Chitosan Porous Materials: A Review of Preparation, Structure Characterization and Application. *Int. J. Mol. Sci.* **2022**, *23*.
31. Saheed, I.O.; Oh, W. Da; Suah, F.B.M. Chitosan modifications for adsorption of pollutants – A review. *J. Hazard. Mater.* **2021**, *408*, 124889.
32. Zhao, X.; Wu, Q.; Huang, C.; Wei, H.; Wang, R.; Wang, C. Highly efficient separation membrane based on cellulose acetate/chitosan fibrous composite substrate with activated carbon functional adsorption layer. *J. Chem. Technol. Biotechnol.* **2021**, *96*, 672–679.
33. Salama, A.; Mohamed, A.; Aboamera, N.M.; Osman, T.; Khattab, A. Characterization and mechanical properties of cellulose acetate/carbon nanotube composite nanofibers. *Adv. Polym. Technol.* **2018**, *37*, 2446–2451.
34. Nandanwar, P.; Jugade, R.; Gomase, V.; Shekhawat, A.; Bambal, A.; Saravanan, D.; Pandey, S. Chitosan-Biopolymer-Entrapped Activated Charcoal for Adsorption of Reactive Orange Dye from Aqueous Phase and CO2 from Gaseous Phase. *J. Compos. Sci.* **2023**, *7*.
35. Karthik, D.; Militky, J.; Wang, Y.; Venkataraman, M. Joule Heating of Carbon-Based Materials Obtained by Carbonization of Para-Aramid Fabrics. *C* **2023**.
36. Saleem, J.; Shahid, U. Bin; Hijab, M.; Mackey, H.; McKay, G. Production and applications of activated carbons as adsorbents from olive stones. *Biomass Convers. Biorefinery* **2019**, *9*, 775–802.
37. Kwa, A. Physical Properties of Starch / Powdered Activated Carbon. *Polymers (Basel).* **2021**.

38. Blachnio, M.; Derylo-Marczewska, A.; Charmas, B.; Zienkiewicz-Strzalka, M.; Bogatyrov, V.; Galaburda, M. *Activated Carbon from Agricultural Wastes for Adsorption of Organic Pollutants*; 2020; Vol. 25; ISBN 4881537563.
39. Sultana, M.; Rownok, M.H.; Sabrin, M.; Rahaman, M.H.; Alam, S.M.N. A review on experimental chemically modified activated carbon to enhance dye and heavy metals adsorption. *Clean. Eng. Technol.* **2022**, *6*, 100382.
40. Liu, M.; Xiao, C. Research progress on modification of activated carbon. *E3S Web Conf.* **2018**, *38*, 2–5.
41. Bhatnagar, A.; Hogland, W.; Marques, M.; Sillanpää, M. An overview of the modification methods of activated carbon for its water treatment applications. *Chem. Eng. J.* **2013**, *219*, 499–511.
42. Alsohaimi, I.H.; Alhumaimess, M.S.; Hassan, H.M.A.; Reda, M.; Aldawsari, A.M.; Chen, Q.; Kariri, M.A. Chitosan Polymer Functionalized-Activated Carbon/Montmorillonite Composite for the Potential Removal of Lead Ions from Wastewater. *Polymers (Basel).* **2023**, *15*.
43. Mobarak, M.; Ali, R.A.M.; Seliem, M.K. Chitosan/activated coal composite as an effective adsorbent for Mn(VII): Modeling and interpretation of physicochemical parameters. *Int. J. Biol. Macromol.* **2021**, *186*, 750–758.
44. Jawad, A.H.; Abdulhameed, A.S.; Surip, S.N.; Sabar, S. Adsorptive performance of carbon modified chitosan biopolymer for cationic dye removal: kinetic, isotherm, thermodynamic, and mechanism study. *Int. J. Environ. Anal. Chem.* **2022**, *102*, 6189–6203.
45. Elmaghraby, N.A.; Omer, A.M.; Kenawy, E.R.; Gaber, M.; Hassaan, M.A.; Ragab, S.; Hossain, I.; El Nemr, A. Electrospun cellulose acetate/activated carbon composite modified by EDTA (rC/AC-EDTA) for efficient methylene blue dye removal. *Sci. Rep.* **2023**, *13*, 1–16.
46. Parthasarathy, P.; Narayanan, S.K. Effect of Hydrothermal Carbonization Reaction Parameters on. *Environ. Prog. Sustain. Energy* **2014**, *33*, 676–680.
47. de Freitas, F.P.; Carvalho, A.M.M.L.; Carneiro, A. de C.O.; de Magalhães, M.A.; Xisto, M.F.; Canal, W.D. Adsorption of neutral red dye by chitosan and activated carbon composite films. *Heliyon* **2021**, *7*.